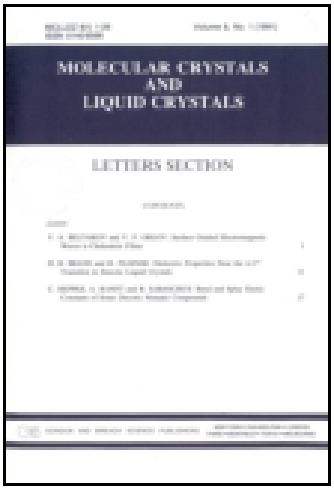

Molecular Crystals and Liquid Crystals
Publication details, including instructions for authors and subscription information:
http://www.tandfonline.com/loi/gmcl20

Exotic Defect Structures and Their Optical Properties in a Strongly Confined Chiral Liquid Crystal

Jun-Ichi Fukuda[abc] & Slobodan Žumer[bcd]
[a] Nanosystem Research Institute (NRI), National Institute of Advanced Industrial Science and Technology (AIST), Tsukuba, JAPAN
[b] Faculty of Mathematics and Physics, University of Ljubljana, Ljubljana, SLOVENIA
[c] Center of Excellence NAMASTE, Ljubljana, SLOVENIA
[d] Jožef Stefan Institute, Ljubljana, SLOVENIA
Published online: 30 Sep 2014.

To cite this article: Jun-Ichi Fukuda & Slobodan Žumer (2014) Exotic Defect Structures and Their Optical Properties in a Strongly Confined Chiral Liquid Crystal, Molecular Crystals and Liquid Crystals, 594:1, 70-77, DOI: 10.1080/15421406.2014.917474

To link to this article: http://dx.doi.org/10.1080/15421406.2014.917474

Mol. Cryst. Liq. Cryst., Vol. 594: pp. 70–77, 2014

ISSN: 1542-1406 print/1563-5287 online
DOI: 10.1080/15421406.2014.917474

Exotic Defect Structures and Their Optical Properties in a Strongly Confined Chiral Liquid Crystal

JUN-ICHI FUKUDA[1,2,3,*] AND SLOBODAN ŽUMER[2,3,4]

[1]Nanosystem Research Institute (NRI), National Institute of Advanced Industrial Science and Technology (AIST), Tsukuba, JAPAN
[2]Faculty of Mathematics and Physics, University of Ljubljana, Ljubljana, SLOVENIA
[3]Center of Excellence NAMASTE, Ljubljana, SLOVENIA
[4]Jožef Stefan Institute, Ljubljana, SLOVENIA

We numerically investigate structural and optical properties of a highly chiral liquid crystal when it is confined in a thin planar cell imposing strong homeotropic anchoring. Various stable exotic defect structures different from those of bulk cholesteric blue phases are found depending on temperature and cell thickness. We also study how a planar cell with these defect structures reflect and transmit incident light, paying particular attention to a structure with double-helix disclination lines and one similar to bulk BP II.

Keywords Chiral liquid crystal; cholesteric blue phase; topological defects; Maxwell equations; reflection

I. Introduction

Absence of inversion symmetry in a chiral liquid crystal gives rise to a rich variety of ordered phases [1]. The simplest example is a chiral nematic (or cholesteric) phase in which the director $\boldsymbol{n}$ rotates (or twists) along one direction. One can consider a configuration of $\boldsymbol{n}$ exhibiting twist distortions along more than one direction, which is referred to as "double twist" and energetically more favorable locally than a "single twist" of a chiral nematic. Cholesteric blue phases (BPs) [1,2], more complex and intriguing ordered phases exhibited by a chiral liquid crystal, comprises this double-twist ordering and disclination lines of winding number $-1/2$ that inevitably appear because of the frustration between the locally favorable double-twist ordering and global topological constraint that prohibits double-twist ordering from filling the whole space without singularities. Not only have cholesteric BPs intrigued scientists as a fascinating example of frustrated systems, but also attracted considerable attention as a possible candidate of materials suitable for next-generation fast-switching displays [3,4].

*Address correspondence to Jun-ichi Fukuda, Nanosystem Research Institute, AIST, 1-1-1 Umezono, Tsukuba 305-8568, JAPAN. Tel.: +81-29-861-3248; Fax: +81-29-861-5375. Email: fukuda.jun-ichi@aist.go.jp

By numerical calculations based on the Landau-de Gennes theory, we have shown [5] that, when a chiral liquid crystal exhibiting cholesteric BPs in the bulk is strongly confined in a planar cell whose thickness is of the order of or smaller than the lattice constant of bulk BPs, it exhibits various exotic ordered structures most of which are considerably different from those of bulk BPs. These structures, which we will present later, include disclination lines of double-helix form, and a quasi-two-dimensional hexagonal lattice of Skyrmion excitations. In this work, we will particularly focus on how these exotic structures respond to incident light. Although optical properties, in particular photonic bands of cholesteric BPs have been theoretically investigated [6,7], lasing of cholesteric BPs has been experimentally demonstrated [8,9], a thin cell of a cholesteric BP liquid crystal has been paid less attention. Given the peculiarity of ordered structures of a chiral liquid crystal confined in a thin cell, one can imagine that these periodic structures can exhibit non-trivial optical properties arising from the anisotropic and inhomogeneous distribution of the dielectric tensor $\overleftrightarrow{\epsilon}$. Here we will investigate the profiles of reflected light and transmitted light when an ordered structure of a chiral liquid crystal in a thin cell is illuminated by light with specific polarization. Our calculations are based on a plane-wave expansion, and one of its advantages over the commonly used finite-difference-time-domain (FDTD) method [10] is that full three-dimensional grids need not be introduced outside the liquid crystal. Another advantage is that one has to include no other ingredients that do not appear in the original Maxwell equations or appropriate boundary conditions (for example, absorbing boundaries to mimic infinite space outside the liquid crystal).

II. Numerical Calculations

A. Calculation of the Order Parameter Profiles

In our numerical calculations to determine the equilibrium orientation profiles of a chiral liquid crystal, we employ the Landau-de Gennes theory in which the orientational order of the liquid crystal is described by a symmetric and traceless second-order tensor $\chi_{\alpha\beta}$ [11]. The details of our calculations are given in our previous works [5] and here we show the outline. After an appropriate rescaling of length, order parameter, and free energy density, the total free energy of the system is formally given by $\mathcal{F} = \int dxdy[\int_0^L(\varphi_{\text{local}} + \varphi_{\text{grad}}) + \varphi_{\text{s0}} + \varphi_{\text{s}L}]$, where L is the thickness of the liquid crystal cell, φ_{local} is the local free energy density as a Landau expansion, φ_{grad} is the elastic energy density, or the contribution from the inhomogeneity of $\chi_{\alpha\beta}$, and $\varphi_{\text{s}0,L}$ is the anchoring energy at the two confining surfaces located at $z = 0, L$ (cell normal is taken along the z direction). The explicit forms of the free energy densities are

$$\varphi_{\text{local}}(\chi_{\alpha\beta}) = \tau\,\text{Tr}\chi^2 - \sqrt{6}\,\text{Tr}\chi^3 + \left(\text{Tr}\chi^2\right)^2, \tag{1}$$

$$\varphi_{\text{grad}}(\chi_{\alpha\beta}, \nabla) = \kappa^2\{[(\nabla \times \chi)_{\alpha\beta} + \chi_{\alpha\beta}]^2 + \eta[(\nabla \cdot \chi)_\alpha]^2\}, \tag{2}$$

$$\varphi_{\text{s}} = \frac{1}{2}w\text{Tr}(\chi - \chi_{\text{s}})^2. \tag{3}$$

Here τ is the temperature, κ is the strength of chirality, and w is the anchoring strength. η concerns the anisotropy of liquid crystal elasticity and is set to 1 corresponding to the one-constant approximation. χ_{s} is the order parameter preferred by the confining surfaces, and in this work it is chosen so that the surfaces impose homeotropic anchoring. The length

is rescaled such that the natural cholesteric pitch p is 4π. We choose $w = 2.5$ (strong anchoring) and $\kappa = 0.7$ (corresponding to $p \simeq 161$ nm in real unit). The equilibrium profile is calculated by relaxing not only $\chi_{\alpha\beta}$ but the lattice constants of the numerical system along the x and y directions to avoid the mismatch between the periodicity of the liquid crystal ordering and the size of the numerical system.

B. Calculation of the Optical Properties

Now we present how we calculate the optical properties of the liquid crystal structures found in Sec. II A . Under the assumption of no current or charge, and that the time dependence of the electric field $\boldsymbol{E}$ and the magnetic field $\boldsymbol{H}$ is described by a single frequency ω as $\propto \exp(-i\omega t)$, the Maxwell equation for $\boldsymbol{E}$ is written as [12]

$$\nabla \times \nabla \times \boldsymbol{E} - \left(\frac{\omega}{c}\right)^2 \overleftrightarrow{\epsilon}\, \boldsymbol{E} = 0, \tag{4}$$

with $\overleftrightarrow{\epsilon}$ being the dielectric tensor.

We consider the cases where light with frequency ω is incident normally from $z = -\infty$, and denote the regions $-\infty < z < 0$, $0 \le z \le L$, and $L < z < \infty$ by Regions 1,2 and 3, respectively (Region 2 is occupied by the liquid crystal). According to the Bloch theorem, $\boldsymbol{E}$ in a periodic medium in the $\boldsymbol{r}_\perp = (x, y)$ directions is formally expanded as $\boldsymbol{E}(\boldsymbol{r}_\perp, z) = \sum_{m,n} \boldsymbol{E}^{(m,n)}(z) \exp\left(i[\boldsymbol{k}_\perp + \boldsymbol{G}_\perp^{(m,n)}] \cdot \boldsymbol{r}_\perp\right)$. Here $\boldsymbol{k}_\perp$ is an arbitrary vector in the (x, y) space, and $\boldsymbol{G}_\perp^{(m,n)}$ is a 2-dimensional reciprocal vector labeled by integers m and n that is consistent with the periodicity of the medium. Since we are considering normal incidence, $\boldsymbol{k}_\perp = 0$. The electric field of the incident light is given by $\boldsymbol{E}(x, y, z) = \boldsymbol{E}_\mathrm{i} \exp(ik_\mathrm{i} z)$, where $\boldsymbol{E}_\mathrm{i} \cdot \hat{\boldsymbol{z}} = 0$ from the transverse condition, and the dispersion relation yields $k_\mathrm{i}^2 = \epsilon_1(\omega/c)^2$, where c is the speed of light in vacuum.

We assume that Regions 1 and 3 are isotropic and homogeneous in terms of dielectric permittivity and the dielectric constants there are denoted by $\epsilon_{1,3}$, respectively. We can safely set $\boldsymbol{E}_{1,3}^{(m,n)}(z) = \tilde{\boldsymbol{E}}_{1,3}^{(m,n)} \exp(ik_{z1,3}^{(m,n)} z)$, and the electric fields in Regions 1 and 3 are expanded in terms of the labels (m, n). Note that $|\boldsymbol{G}_\perp^{(m,n)}|^2 + (k_{z1,3}^{(m,n)})^2 = \epsilon_{1,3}(\omega/c)^2$, and therefore k_{z1} and k_{z3} are pure imaginary if $|\boldsymbol{G}_\perp^{(m,n)}|^2 > k_\mathrm{i}^2$, and $|\boldsymbol{G}_\perp^{(m,n)}|^2 > (\epsilon_3/\epsilon_1)k_\mathrm{i}^2$, respectively. Imaginary $k_{z1,3}$ gives rise to an evanescent wave.

In Region 2, the dielectric tensor is inhomogeneous and anisotropic because of the ordered structure of the liquid crystal, and therefore the z dependence of the electric field cannot in general be given by a single exponential function as in Regions 1 and 3. We simply discretize $\boldsymbol{E}$ in the z direction so that it is formally written as $\boldsymbol{E}_2(\boldsymbol{r}_\perp, z_l) = \sum_{m,n} \boldsymbol{E}_2^{(m,n,l)} \exp(i\boldsymbol{k}_\perp^{(m,n)} \cdot \boldsymbol{r}_\perp)$, where z_l's ($l = 0, 1, \ldots, l_\mathrm{max}$) with equal spacings satisfy $0 = z_0 < z_1 < \cdots < z_{l_\mathrm{max}} = L$. We further assume that the dielectric tensor is given, as a function of $\chi_{\alpha\beta}$ by $\epsilon_{\alpha\beta}(\boldsymbol{r}) = \epsilon_\mathrm{iso}\delta_{\alpha\beta} + \epsilon_\mathrm{a}\chi_{\alpha\beta}(\boldsymbol{r})$, and that $\epsilon_{\alpha\beta}(\boldsymbol{r})$ can be discretized in the same manner as $\boldsymbol{E}_2$. The discretization along the z is carried out so that the energy conservation is satisfied in the sense that the sum of transmittance and reflectance is exactly 1 up to rounding errors [13].

After the plane-wave expansion is truncated by limiting m and n, the discretization of eq. (4) together with appropriate boundary conditions at the surfaces confining the liquid crystal results in a set of linear equations for given $\boldsymbol{E}_\mathrm{i}$ and k_i. The number of equations is exactly the same as that of unknowns: $\tilde{\boldsymbol{E}}_{1,3}^{(m,n)}$ and $\boldsymbol{E}_2^{(m,n,l)}$. In the present calculations we set $l_\mathrm{max} = 32$ and $-16 \le m, n \le 16$. We retain only dominant $\overleftrightarrow{\epsilon}^{(m,n,l)}$'s to reduce numerical

costs (how many $\overleftrightarrow{\epsilon}^{(m,n,l)}$'s out of 33^2 are retained depends on the problems, and for the calculation presented in Section III B below, 81 and 59 modes are retained for two different structures). Then our linear equations are sparse enough to be handled by a direct solver UMFPACK [14] designated for sparse linear equations.

As material parameters, we choose $\epsilon_{1,3} = 2.25$, and the corresponding refractive index 1.5 is typical for glass. $\epsilon_{\rm iso}$ and $\epsilon_{\rm a}$ are set to 2.571 and 0.825, respectively, that conform to the refractive indices of a typical blue phase material $n_\parallel = 1.754$ and $n_\perp = 1.523$ [15].

III. Results

A. Defect Structures in a Thin Cell

In Fig. 1 we show stable or metastable defect structures in a thin planar cell of a chiral liquid crystal, found in our numerical calculations [5]. Figure 1 clearly demonstrates that, merely by changing cell thickness L and temperature τ, the system can exhibit various types of defect structures entirely different from those of bulk BPs, except that of Fig. 1(d) resembling that of bulk BP II with four-arm junctions of defects. These exotic defect structures include a hexagonal lattice of Skyrmion excitations (Fig. 1(a)), intricate disclination network with apparent three-fold symmetry (Fig. 1(b)) or rectangular symmetry (Fig. 1(c)), a parallel array of disclination lines with double-helix form (Fig. 1(e)), and a staggered array of inchworm-like disclination lines in contact with confining surfaces (Fig. 1(f)). Notice that Skyrmions, vortex-like excitations in vectorial order originally proposed to account for the existence of discrete entities in a continuous field theory for elementary particles [16], have

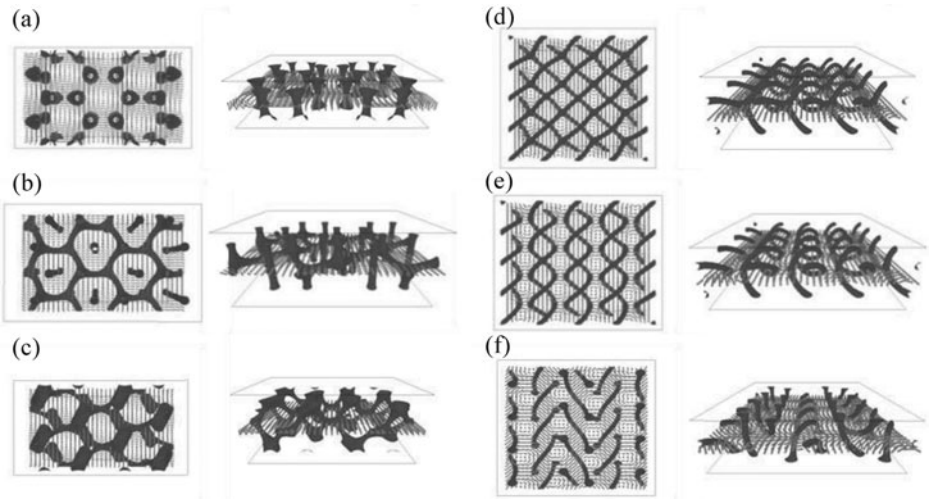

Figure 1. Defect structures of a chiral liquid crystal confined in a thin planar cell with strong homeotropic anchoring. Profiles of topological disclination lines are shown by isosurfaces of $\mathrm{Tr}\chi^2$, and the orientation profiles at the midplane are shown by small cylinders. The (rescaled) cell thickness L and temperature τ are (a) $L/p = 0.637$, $\tau = 0$, (b) $L/p = 0.955$, $\tau = 0$, (c) $L/p = 0.955$, $\tau = 0.2$, (d) $L/p = 1.114$, $\tau = -0.6$, (e) $L/p = 0.955$, $\tau = -0.6$ and (f) $L/p = 0.796$, $\tau = -0.6$, respectively. Here $p = 4\pi$ is the rescaled cholesteric pitch. Note that surface defects are not shown for the clarity of the top views.

attracted considerable interest in diverse fields of physics and shown to play an important role in, say, two-dimensional electron gases, spinor Bose-Einstein condensates, and chiral ferromagnets [17].

We can show that these defect structures are indeed stable in a certain space in the (L, τ) space. The phase diagram is presented in our previous work [5].

B. Optical Properties

In this work we pay particular attention to two of the defect structures presented in Section III A; a BP II like structure with an array of four-arm junction of defects which we will refer to as "BP II-like" in the following (Fig. 1(d), $L/p = 1.114$), and a parallel array of disclinations of double-helix form referred to as "double-helix" (Fig. 1(e), $L/p = 0.955$).

In Fig. 2 we show the reflectance as a function of the wavelength of the incident light in Region 1, which will be denoted by λ_i ($\epsilon = 2.25$ and the refractive index is 1.5 there, and therefore λ_i is 1.5 times smaller than that in vacuum). We focus on the effect of the handedness of circular polarization on the reflectance. For both structures, the reflectance of right-handed circular polarized light is much larger than that of left-handed polarized light for almost the whole range of the wavelength. The reflectance for right-handed polarized light can be about 0.9, while it is at most 0.2 for "BP II-like," and 0.45 for "double-helix" when the polarization is left-handed. This difference is clearly attributed to the absence of inversion symmetry of the structure of the system, as is well known for a helical orientation profile of a chiral nematic [11].

In Fig. 3, we show the profiles of $\boldsymbol{E}^* \cdot \boldsymbol{E}$ of reflected light for different z's, where $\boldsymbol{E}^*$ is the complex conjugate of $\boldsymbol{E}$. We have chosen $\lambda_i = 7.947$ for "BP II-like" and 8.840 for "double-helix," both of which give a local peak in the reflectance spectra. Despite the in-plane variations of orientational order for both structures, the intensity profiles look almost one-dimensional; the variation along one direction (that of the helical axes of disclination lines for "double-helix") decays rapidly with the distance from the confining surface $|z|$. Stripe-like appearance of the intensity profiles is common for both structures. The rapid decay to stripe-like profile looks surprising, in particular for the BP II-like structure, and it could be attributed to the presence of stripe-like surface defects not shown in Fig. 1 for the clarity of the presentation. The intensity profiles for a given structure of the liquid crystal and a given $|z|$ look almost the same irrespective of the polarization of the incident light

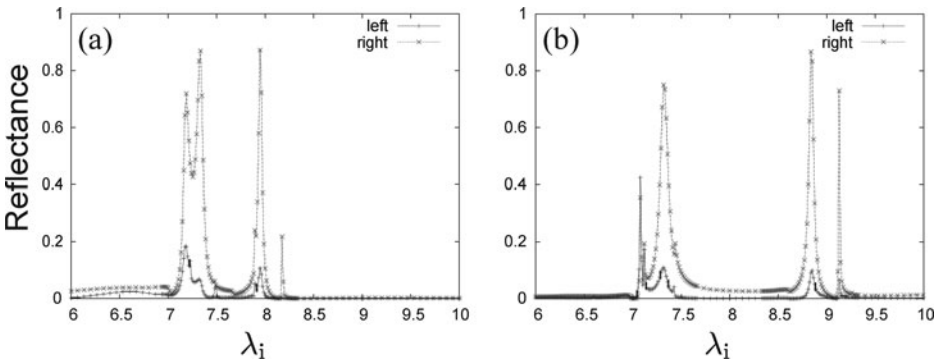

Figure 2. Reflectance spectra for (a) "BP II-like" and (b) "double-helix" structures. λ_i is the wavelength of the incident light in Region 1.

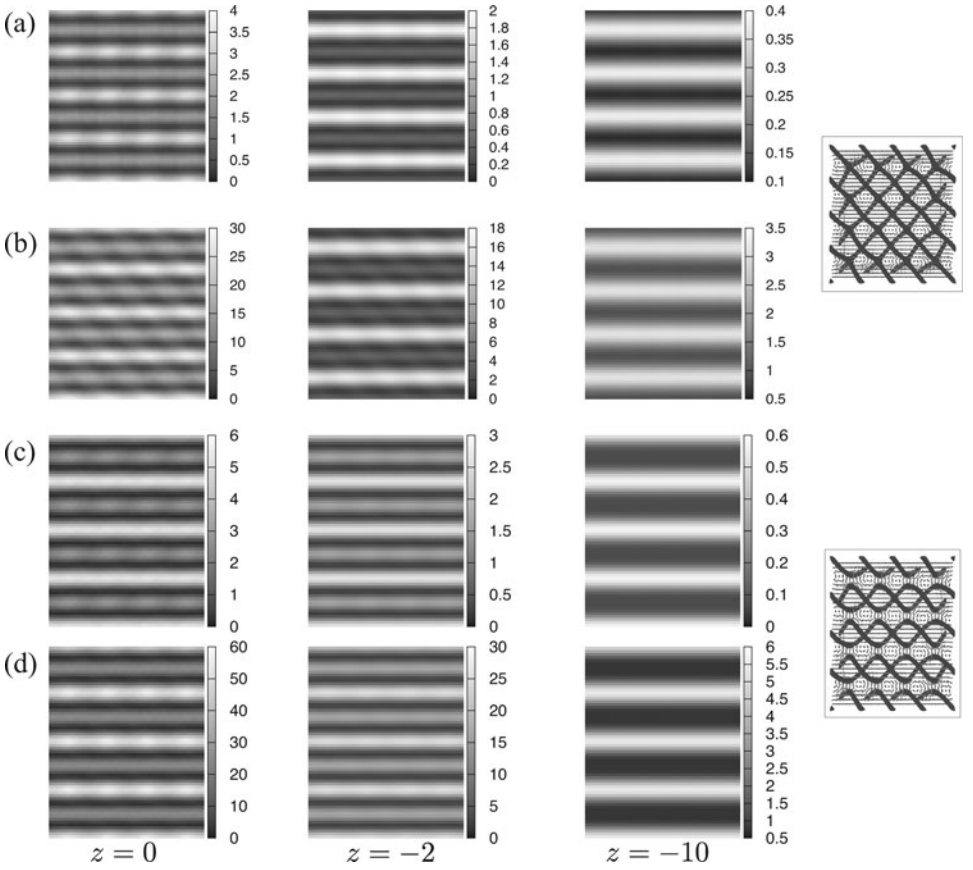

Figure 3. Intensity ($\boldsymbol{E}^* \cdot \boldsymbol{E}$) profiles of reflected light for (a,b) "BP II-like" (the area shown is 14.34×15.76.) and (c,d) "double-helix" structures (the area shown is 14.25×17.67.) at $z = 0, -2$ and -10. The length is rescaled so that the natural cholesteric pitch ($\simeq$161 nm) becomes 4π. The polarization of the incident light is left-circular for (a,c) and right-circular for (b,d). The defect structures are also shown to clarify the orientation of the intensity profiles with respect to the structure of the liquid crystal.

(left-circular or right-circular). However, the intensity scales in Fig. 3 again clearly indicate that the intensity of reflected light is much stronger for right-circular incident light. We also note that for the present choice of λ_i, all the modes $\boldsymbol{E}_1^{(m,n)}$ with nonzero $\boldsymbol{G}_\perp^{(m,n)}$ are evanescent (in other words, $k_{z1}^{(m,n)}$ is pure imaginary), and therefore the intensity profiles become uniform for large $|z|$ (the decay of the amplitude of intensity modulation can be seen in the intensity scales of Fig. 3).

IV. Conclusion

We presented our numerical work on the formation of exotic defect structures in a chiral liquid crystal strongly confined between two parallel plates. Depending on temperature and the thickness of the system, the liquid crystal exhibits a wide variety of defect structures not found in other systems including bulk cholesteric BPs. These exotic structures include a hexagonal lattice of Skyrmion excitations, a bulk BP II-like structure with four-arm junctions of disclination lines, and a parallel array of disclination lines of double-helix form.

These results clearly demonstrates that liquid crystals have possibilities of self-organized structure formation much more than we already know or we can imagine now.

We also showed some results of our numerical work on the optical properties of these exotic defect structures. By plane-wave expansions, we investigated how our thin system with an inhomogeneous distribution of the dielectric tensor $\overleftrightarrow{\epsilon}$ reflects and transmits monochromatic light incident normally. In this work we particularly focused on two structures, one similar to that of bulk BP II, and a parallel array of disclination lines of double-helix form. We showed clear dependence of the reflection intensity spectrum on the polarization of incident light, which resembles the response of a chiral nematic with single twist, and reflects the lack of inversion symmetry in our system of a chiral liquid crystal. Though the in-plane structures of the liquid crystal vary in two dimensions, the intensity profile of the reflected light is of a stripe form. Our results are preliminary in the sense that we focused on a small number of structures and presented only the intensity profiles for incident light of specific wavelengths. Nevertheless, we believe that a thin system of a chiral liquid crystal exhibiting various exotic defect structures is not only a playground for theoretical analyses but also will be useful as a tunable optical grating. Our present work based on plane-wave expansions will be a starting point for a further study of optical properties of such systems.

Acknowledgments

We thank Dr. Andrij Nych for showing us his preliminary experimental results and valuable discussions, which motivated the latter part of this work. This work was supported by the Slovenian Research Agency (ARRS research program P1-0099 and project J1-2335), and the Center of Excellence NAMASTE, which enabled J.F. to stay at the University of Ljubljana and carry out the significant part of this work there. J.F. was also supported by JSPS KAKENHI (Grant Number 25400437) and the Cooperative Research Program of "Network Joint Research Center for Materials and Devices."

References

[1] Kitzerow, H. S., & Bahr, C. (ed.). (2001). *Chirality in Liquid Crystals*, Springer: Berlin.
[2] Wright, D. C., & Mermin, N. D. (1989). *Rev. Mod. Phys.*, *61*, 385.
[3] Kikuchi, H., Higuchi, H., Haseba, Y., & Iwata, T. (2007). *SID Symposium Digest of Technical Papers*, 38, 1737.
[4] Ge, Z., Gauza, S., Jiao, M., Xianyu, H., & Wu, S. T. (2009). *Appl. Phys. Lett.*, *94*, 101104.
[5] Fukuda, J., & Žumer, S. (2010). *Phys. Rev. Lett.*, *104*, 017801; *Liq. Cryst., 37,* 875 (2010); *Phys. Rev. Lett., 106,* 097801 (2011); *Nature Commun., 2,* 246 (2011).
[6] Hornreich, R. M., Shtrikman, S., & Sommers, C. (1993). *Phys. Rev. E*, *47*, 2067.
[7] Ojima, M. *et al.* (2010). *Appl. Phys. Express*, *3*, 032001; Y. Ogawa *et al., Optics Letters, 38,* 3380 (2013).
[8] Cao, W., Muñoz, A., Palffy-Muhoray, P., & Taheri, B. (2002). *Nat. Mater.*, *1*, 111.
[9] Yokoyama, S., Mashiko, S., Kikuchi, H., Uchida, K., & Nagamura, T. (2006). *Adv. Mater.*, *18*, 48.
[10] Taflove, A., & Hagness, S. C. (2005). *Computational Electrodynamics, The Finite-Difference Time-Domain Method,* 3rd ed, Artech House Publishers.
[11] de Gennes, P. G., & Prost, J. (1993). *The Physics of Liquid Crystals,* 2nd ed, Oxford University Press: Oxford.
[12] Landau, L. D., Lifshitz, E. M., & Pitaevskii, L. P. (1984). *Electrodynamics of Continuous Media* (2nd ed.), Butterworth-Heinemann.

[13] Dossou, K. B., & Botten, L. C. (2012). *J. Comp. Phys.*, *231*, 6969.
[14] Davis, T. A. (2004). *ACM Transactions on Mathematical Software*, *30*, 196.
[15] Nych, A. (private communication).
[16] Skyrme, T. (1962). *Nucl. Phys.*, *31*, 556.
[17] Brown, G. E., & Rho, M. (ed.). (2010). *The Multifaceted Skyrmion*, World Scientific: Singapore.